Vibration Energy Harvesting for Wireless Underground Sensor Networks

Salman Kahrobaee*
* Department of Electrical Engineering
University of Nebraska-Lincoln, Lincoln, NE 68588
Email: skahrobaee@huskers.unl.edu

Mehmet C. Vuran†
† Department of Computer Science & Engineering
University of Nebraska-Lincoln, Lincoln, NE 68588
Email: mcvuran@cse.unl.edu

***Abstract*—Recent developments in wireless underground communication have enabled the realization of underground sensor network applications. To this end, it is desirable to provide a sustainable operation for wireless underground sensor networks (WUSNs) with extended lifetimes as maintenance is significantly costly. One promising method towards sustainable operation is to harvest energy underground based on the vibration sources in the environment. However, to the best of our knowledge, underground vibration energy harvesting has not been investigated before. In this paper, the feasibility of vibration energy harvesting for WUSNs is investigated. First, an analytical framework is developed to model the maximum harvestable power by a piezoelectric energy harvester at a certain depth underground, due to an aboveground vibration source. Then, field experiments are conducted to measure the vibration in an agricultural testbed and evaluated the harvestable output power. The results from this study illustrate the feasibility of vibration energy harvesting as a promising approach to be considered for the future underground sensor networks.**

I. Introduction

Wireless underground sensor networks (WUSNs) is a promising and evolving area within wireless sensor networks (WSN) [1]. Applications of WUSNs are valuable in a wide range including sports fields, agriculture, precision irrigation, environmental monitoring, border patrol, and structural health monitoring [1], [3], [5], [22], [28].

In practice, however, there are a number of challenges to address for the proliferation of WUSN applications [1]. In a WUSN, the communication is established through the soil in which electromagnetic waves encounter much higher attenuation than in air [18], [19]. In addition, the communication is dynamically affected by the changes in the characteristics of the soil such as its moisture, and temperature [25]. Therefore, recently, there have been a number of studies to model the characterization of the communication channel, and perform empirical analysis of the WUSNs [5], [6], [12], [18], [25].

Another challenge in WUSNs is to provide sustainable energy for the deployed sensors. Depending on the application, WUSN devices should have a lifetime of at least several years to make their deployment cost-efficient [23]. Despite the ongoing improvements and conservations made by utilizing energy-efficient hardware and communication protocols, the power consumption due to communicating through the soil is still significant. In addition, within a WUSN infrastructure, the power source of the sensors may not be easily accessible for maintenance or replacement when they are buried in the ground.

In general, there are two solutions to supply power for *underground* sensor networks:

1) **Wireless Power Transfer:** A number of methods may be used to transfer the energy wirelessly such as electromagnetic induction, radiation, or electromagnetic resonance [4], [8]–[10].
2) **Energy Harvesting:** Energy harvesting components can be integrated to underground sensor nodes to harvest energy from the natural sources of energy in the environment. There are a couple options to choose from such as underground living plants and bacteria to be used in a fuel cell [21] or vibration energy harvesting [15], [16].

The wireless power transfer methods have mainly been investigated for mobile and above ground applications. However, there are several restrictions for these methods in WUSN applications, mainly because an adequate energy resource should be available aboveground. This requires a facility to be built up for the aboveground power source which otherwise should be carried to the network area on a regular basis, such as using a flying object. In addition, the efficiency of wireless power transfer techniques in soil is not well understood. On the other hand, energy harvesting is promising since the energy harvester can be deployed underground to exploit *existing* vibration sources. Therefore, no *dedicated* aboveground interaction is needed. Examples of vibration sources include agricultural machinery in agricultural applications and vehicles in road monitoring applications.

Among the energy scavenging methods, vibration energy harvesting has recently been considered in traditional WSN applications [15], [16]. In this method, power is generated based on a piezoelectric element that converts the vibration into electricity. Piezoelectric energy harvesters can be seen as an equivalent mechanical model using spring, mass, and damper [27], or modelled based on their equivalent circuit model [26]. In general, the main concern with vibration energy harvesting is whether this method is able to provide sufficient energy for the desired application. In addition, piezoelectric has a frequency response, and it should be tuned to the right frequency to generate its expected power. Then, the challenge with using piezoelectric in an environment, where a wide range of vibration frequencies is observed, is to obtain the right frequency which generates the highest output. A number of studies have addressed these issues by analyzing and testing

the output power of piezoelectric energy harvesters [7], [14], [17], [20]. However, none of these methods has focused on underground applications and the vibration energy harvesting in soil has not been analyzed to the best of our knowledge.

In this paper, we investigate the scenario where piezoelectric energy harvesters are used as power sources for WUSNs applications. Depending on the location, there may be several vibration sources for WUSNs. For example, in an agricultural field, mobile irrigation systems, seeders, harvesters, combines, and other agricultural machines could be sources of vibration. Then, the vibration generated above ground should propagate into the soil and reach out to a buried piezoelectric energy harvester. The total power generated by a piezoelectric energy harvester depends on the amount of vibration at the depth of deployment. Therefore, it is necessary to consider the propagation of vibrations into the soil. Through a three-step analysis, we model the output power of an underground energy harvester as a function of the source vibration, piezoelectric parameters, and soil characteristics. In addition, we evaluate underground vibration energy harvesting through field experiments to measure the underground vibration and evaluate the expected harvestable energy in an agricultural field subject to different vibration sources.

The rest of the paper is organized as follows: In Section II, a theoretical analysis is presented for the harvestable underground power as a result of aboveground vibrations. This analysis is evaluated through a case study in an agricultural field as described in Section III, where the procedure for sensor calibration is also described. The results of underground vibration measurements are provided in Section IV. Finally, the paper is concluded in Section V.

II. Theoretical Analysis

Vibration can be defined as mechanical oscillations around an equilibrium point. These oscillations may be expressed by displacement and frequency of the vibrating object. This section provides a mathematical model to calculate the output power of an underground piezoelectric energy harvester at a depth of d_h with an aboveground vibration source as illustrated in Fig. 1.

The analysis consists of three steps. In the first step, the amount of vibration made on the ground surface is formulated. Then, the amount of vibration that is propagated into the soil is modeled. Finally, the amount of electric power generated from this underground vibration at an underground piezoelectric energy harvester is captured.

A. Vibration on Ground Surface

The aboveground vibration-generating foundation applies the force F, which faces a reaction from the soil. As a result, a vertical displacement is created on the soil surface, i.e., footing. By Newton's law of motion, this can be expressed as:

$$F - pA = M\frac{d^2z}{dt^2} \ , \tag{1}$$

where M is the mass of the foundation, A is the area of the footing, the pressure between the foundation mass and the soil is denoted by p, and z denotes the vertical displacement of the footing.

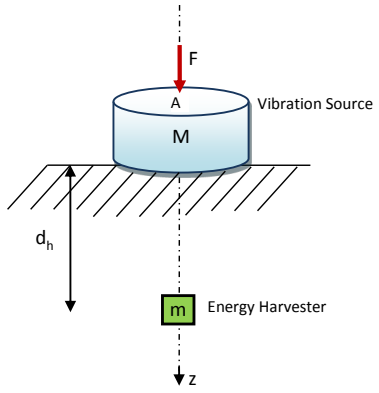

Fig. 1: A vibration source on the surface and a vibration energy harvester in the soil.

Assuming that the applied force, the soil reaction, and the displacement are all periodic, with an angular frequency of ω, (1) can be written as

$$F_0 = p_0A - \omega^2 M z_0 \ , \tag{2}$$

where the index of zero is used for phasor representation of the parameters and by [24]

$$p_0A = (K + i\omega C)z_0 \ , \tag{3}$$

where K and C are dynamic stiffness and dynamic damping of the soil, respectively. These parameters depend on the angular frequency ω, and soil parameters such as shear modulus and soil density as discussed in Appendix A. The dependency of K and C on the frequency can be ignored if ω is relatively smaller than the system characteristic frequency ω_c [24]. By substituting p_0A in (3) into (2), the magnitude of the displacement can be written as

$$|z_0| = \frac{|F_0|}{\sqrt{(K - \omega^2M^2)^2 + (\omega C)^2}} \ . \tag{4}$$

B. Vibration Propagation through Soil

Vibration can be modelled as waves that propagate through the soil. These waves attenuate in soil due to two main factors:

- Expansion of waves, i.e., geometrical attenuation
- Dissipation of energy within the soil, i.e., material damping

Based on these two effects, the attenuation of the vibration from point *a* to point *b* is expressed by [2]:

$$|z_b| = |z_a| \left(\frac{d_a}{d_b}\right)^{\gamma} e^{\frac{\beta\omega}{2}(d_a - d_b)} \ , \tag{5}$$

where d_a and d_b are the depths of point *a* and *b*, respectively, γ is the propagation coefficient, and β is the damping coefficient of the material. Assumption of Rayleigh wave propagation implies that $\gamma = 0.5$. Otherwise, this parameter should be determined by experiment. The range of the damping coefficient, β, for different types of soil is shown in Table I for distances expressed in meters [2].

TABLE I: Typical β values for different types of soil [2]

Class	Type of Material	β
I	Weak or soft soil	6.6×10^{-4} - 20×10^{-4}
II	Competent soil	20×10^{-5} - 6.6×10^{-4}
III	Hard soil	20×10^{-6} - 20×10^{-5}
IV	Competent rock	$< 20 \times 10^{-6}$

In WUSNs, the sensors are generally deployed close to the surface, e.g., in 10cm - 1m depth [5]. Hence, the geometrical attenuation can be safely ignored due to relatively short distance between the vibration source and the location of energy harvesters. Accordingly, using (4) and (5), the magnitude of displacement,$|z_h|$, at the depth of energy harvester, d_h, can be represented as

$$|z_h| = \frac{|F_0|}{\sqrt{(K-\omega^2 M)^2 + (\omega C)^2}} e^{\frac{\beta\omega}{2}(-d_h)} . \quad (6)$$

C. Generated Power

Finally, the maximum amount of power that can be derived from an underground piezoelectric energy harvester is obtained. The mechanical model of a piezoelectric energy harvester consists of mass, piezoelectric component, spring, and damper [7], [27].

The force magnitude, $|F_h|$, applied to the piezoelectric as a result of the displacement can be expressed as:

$$|F_h| = \omega^2 m |z_h| , \quad (7)$$

where m is the mass of piezoelectric. By combining (6) and (7), the force magnitude can be represented as:

$$|F_h| = \omega^2 m \frac{|F_0|}{\sqrt{(K-\omega^2 M)^2 + (\omega C)^2}} e^{\frac{\beta\omega}{2}(-d_h)} . \quad (8)$$

The maximum harvested power of a piezoelectric energy harvester can be estimated by [11] $P_{max} = |F_h|^2/(8c)$, where c is the damping coefficient of the energy harvester representing mechanical loss and friction. Consequently, using (8), the maximum harvestable power can be calculated by

$$P_{max} = \frac{\omega^4 (m)^2}{8c} \times \frac{|F_0|^2}{(K-\omega^2 M)^2 + (\omega C)^2} e^{\beta\omega(-d_h)} . \quad (9)$$

It can be seen from (9) that the maximum harvestable power from an underground piezoelectric harvester is a function of the magnitude and frequency of vibration force, depth of the harvester, soil material, and energy harvester characteristics.

D. Numerical Example

A numerical example is provided to illustrate how the value of P_{max} changes as a function of ω, M, and the depth of the harvester. The values of parameters used in this example are provided in Table II, where some typical values were selected for the piezoelectric parameters, based on related studies [7], [11].

According to (9) and the values in Table II, the maximum estimated power is found to be

$$P_{max} = \frac{5 \cdot 10^{-4} \times \omega^4 |F_0|^2 \times e^{-10^{-4}\omega}}{(168.7 \cdot 10^3 \frac{\omega}{tan(\omega/390)} - M\omega^2)^2 + (168.7 \cdot 10^3 \omega)^2} \quad (10)$$

TABLE II: Parameters used for the numerical example

$m(g)$	$c(N \times s/m)$	β
20	0.1	2×10^{-4}
$d_h(cm)$	K	C
50	$\frac{168.7\omega \times 10^3}{tan(\omega/390)}$	168.7×10^3

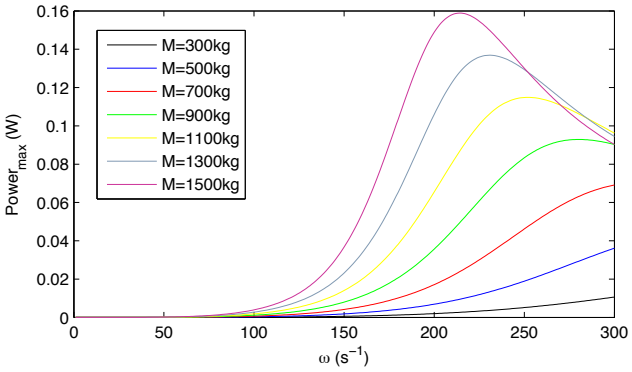

(a)

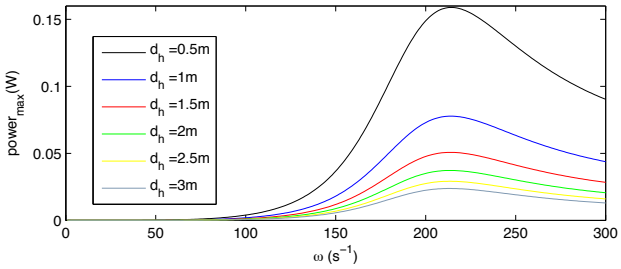

(b)

Fig. 2: Maximum harvested power as a function of angular frequency with (a) different masses ($d_h = 50cm$) and (b) different depths ($M = 1,500$ kg).

In Fig. 2(a), P_{max} is shown as a function of ω with different values of vibration source masses, where the external force is assumed to be caused by the weight of the masses.

As depicted in Fig. 2(a), and according to the parameters of the system, there is a specific frequency where the vibrations can lead to the peak power generation. This indicates the frequency at which the piezoelectric energy harvester should be tuned.

The effect of burial depth is shown in Fig. 2(b) for a mass of $M = 1,500$ kg. It is important to note that as the depth increases, the effect of wave propagation cannot be ignored. Therefore, we include the effect of depth based on (5) using the vibration at the depth of 0.5 m as a reference. It can be observed that the magnitude of harvestable power diminishes with depth due to attenuation. However, the peak power frequency does not change as it depends on the mass.

III. Experiment Setup

The case study of this research is an agricultural field where we measure the vibrations underground to evaluate the expected harvestable energy for a WUSN. In this section, we describe the calibration of the accelerometer sensor used for vibration measurement, and introduce the setup used for the experiments.

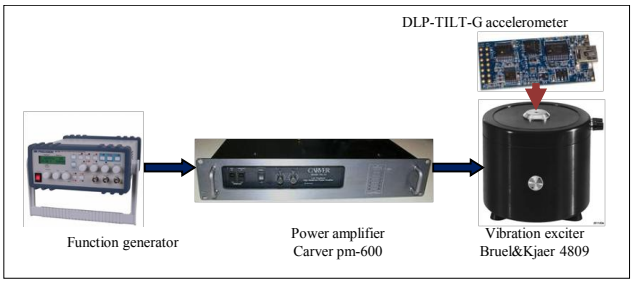

Fig. 3: Schematic of the devices used for the accelerometer calibration experiments.

A. Sensor Calibration

The sensor used for the experiment is DLP-TILT-G, which is a USB-based tilt sensor and 1.5g accelerometer with a range of sampling rate from 100 to 6,000 samples per second. We use MATLAB to read the stream of the acceleration measurements and sketch the FFT graphs.

Before using the accelerometer, it should be calibrated by mapping its output measurements to the corresponding vibration. In Fig. 3, the schematic of the devices used for this experiment is shown. The function generator is used to generate sinusoidal signals at different frequencies. These signals are amplified by the power amplifier to be adjusted in the range of input power for the vibration exciter (1-5 amps). The accelerometer is pasted to the disk on top of the vibration exciter. The sampling frequency of the sensor has been set to 1kHz, which is sufficient for the frequency range of our studies.

For calibration, the vibration frequency was altered between 2 Hz to 10 Hz with 2 Hz intervals and sensor outputs were recorded. The output trend can be effectively expressed by fitting the results to a second-degree polynomial function as

$$SO = 0.14f^2 + 0.6f + 0.79 \tag{11}$$

where SO and f represent the sensor output and the vibration frequency, respectively.

Accordingly, the relationship between the sensor output and the vibration can be derived. We start by modeling the acceleration. Denoting z_h and a_h as the displacement and acceleration due to the vibration, respectively, a_h can be represented as

$$a_h = -\omega^2 z_h = -(2\pi f)^2 z_h \tag{12}$$

In the calibration experiments, $z_h = 4$mm based on the characteristics of the vibration exciter. By substituting f in (12) into (11), the acceleration due to the vibration, a_h, is calculated as a function of the sensor output

$$a_h = \left(1.1SO - 1.8\sqrt{SO - 0.14} + 0.57\right)/g \tag{13}$$

Accordingly, the acceleration with respect to the measured output of the sensor is shown in Fig. 4. It can be observed that the acceleration can be modeled based on the sensor output, SO, for output values higher than 2. Theoretically, the results are not valid for $SO < 0.14$ because of the square root term in the numerator in (13). Moreover, in practice, the sensor output values less than 5 are not considered because the sensor did not respond to low frequencies during the calibration tests. For the experiments, Fig. 4 was used to calculate the acceleration values from the measured output data of the sensors.

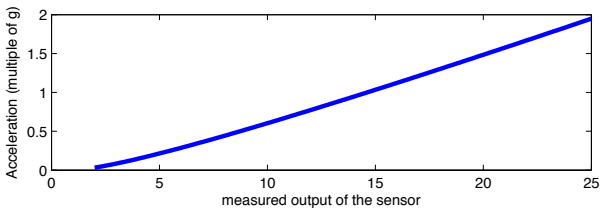

Fig. 4: Acceleration as a function of the sensor output.

Fig. 5: Deployment in a center pivot-irrigated agricultural field.

B. Case Study

To evaluate the underground vibration harvesting, several experiments were performed in an agricultural field located in South Central Agricultural Laboratory, one of the agricultural research divisions (ARD) near Clay Center, Nebraska. The experiments were conducted to measure the magnitude and frequency of the vibrations of agricultural machines including a center pivot irrigation system and a four-wheeler that is frequently used on farms. The vibrations at different depths were measured to evaluate the feasibility of underground energy harvesting.

The experiments were run using 3 DLP-TILT-G accelerometers, two of which were placed vertically at two depths of 20 cm and 40 cm underground, and the third one was placed at a 2 m horizontal distance from the first sensor and at the depth of 20 cm as shown in Fig. 5. Center pivot moves using tires placed at various distances from the center. The sensors in this experiment are buried next to the closest tire to the center. A 4-wheeler is also used at a distance of 1m from the sensors.

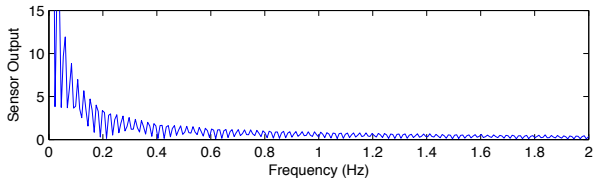

(a) Depth, $d_h = 40$ cm

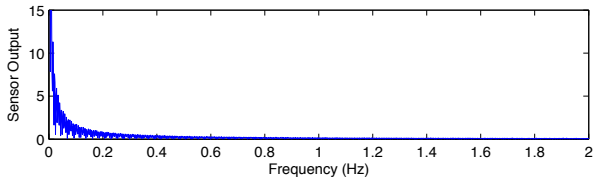

(b) Depth, $d_h = 20$ cm, Distance 2 m

Fig. 6: FFT plot of the center pivot vibrations measured (a) below the tire and (b) 2 m from the tire.

IV. Experiment Results

The vibration was measured simultaneously at all three sensors while the irrigation center pivot was running. In Fig. 6(a), the FFT of the vibration at a depth 20 cm close to the center pivot tire is shown. The sensor at a 40 cm depth was also observed to exhibit a similar response. In Fig. 6(b), the FFT of vibrations for at a distance of 2 m from the tire at a depth of 20 cm is depicted. As expected, this sensor reports even lower vibrations since the sensor is located farther from the vibration source.

Although some vibrations are observed in Fig. 6(a) and Fig. 6(b), the magnitude of vibrations is small, and no specific frequency for the vibration is recognized. This result is mainly due to the relatively smaller vibrations generated by the center pivot and very slow movement of the tire. One complete rotation of the arm of this center pivot takes about 8 hours. Therefore, center pivot may not be a good source of vibration for underground energy harvesting.

The experiment was repeated with a 4-wheeler, which is typically used on agricultural fields for transportation, as the vibration source. The car was parked within a 1 m horizontal distance from the sensors. In Fig. 7, the vibrations measured at depths of 20 and 40 cm are shown when the car engine was on. The main frequency of vibration is 0.24 Hz at which the vibration magnitude is 9.5. The results are similar to those reported in [27], where vibrations from cars on a street were measured.

The magnitude of the vibrations measured at depth 40 cm is 5% less than the results at depth 20 cm with the same frequency. Using the output value at 40 cm, the equivalent acceleration for the main frequency is 0.6g according to Fig. 4. Then, using the parameters of an energy harvester based on Table II, the maximum harvestable power can be calculated using (9), as follows

$$P_{max} = (0.02 \times 0.6 \times 9.8)^2/(8 \times 0.1) = 17mW \qquad (14)$$

The resulting harvestable power is suitable for the application of WUSNs. It can be observed that the generated power is on the order of communication power, which constitutes

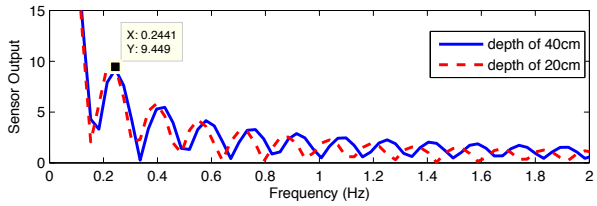

Fig. 7: 4-wheeler vibrations measured at depths 20 cm and 40 cm.

the majority of the energy consumption for WUSNs [23]. Accordingly, for low data-rate applications, vibration energy harvesting can provide sustainable underground operation.

V. Conclusions and Future Work

In this paper, the vibration energy harvesting solution is studied for underground sensor networks applications. Using an analytical approach, the vibration penetration through the soil and expected power achievable at the depth of a piezoelectric energy harvester deployment are analyzed. As a case study, the amount of vibrations from a center pivot irrigation system and a 4-wheeler were measured in an agricultural field, and the harvestable power were calculated. The results indicate that vibration energy harvesting is a promising method for sustainable operation in WUSNs. This method is especially suitable for deployments where aboveground vibration sources exists, such as agriculture operations and road monitoring.

It is important to note that the measured vibration frequency of 0.24 Hz is lower than the practical range of commercial vibration energy harvesters. Moreover, the theoretical harvestable power of 17mW may not be achieved in practice. For example, in [7], an energy harvester is experimentally shown to achieve up to 3.5mW and generate 1.5mW with an acceleration of 0.6g, which is the value observed in our underground experiments. Consequently, higher values of acceleration are required for practical vibration energy harvesting, such as those from seeders, sprayers, and harvesters. Moreover, the effects of various vibration sources in addition to those considered in this work as well as varying environmental conditions such as rain and temperature changes should be studied, which is part of the future work.

Appendix A
Calculation of K and C

The parameters K and C in (3) are dynamic stiffness and dynamic damping of the soil, respectively. For the response of a confined elastic half-space due to a uniform load on a circular area, these parameters can be approximately derived as [24]:

$$K = \frac{(\lambda + 2\mu)\pi a}{n} \times \frac{\omega/\omega_c}{tan(\omega/\omega_c)}, \qquad (15)$$

$$C = \frac{(\lambda + 2\mu)\pi a}{n\omega_c}, \qquad (16)$$

where λ and μ are the elastic coefficients of the soil material (Lam'e constants), a is the radius of the circular area, and n is a material constant defined by:

$$n = \sqrt{\lambda + 2\mu/\mu}\,. \qquad (17)$$

TABLE III: Modulus of elasticity for different types of soil [13]

Soil	E (kPa)
very soft clay	500-5,000
soft clay	5,000-20,000
medium clay	20,000-50,000
stiff clay, silty clay	50,000-100,000
sandy clay	25,000-200,000
clay shale	100,000-200,000
loose sand	10,000-25,000
dense sand	25000-100000
dense sand and gravel	100,000-200,000
silty sand	25,000-200,000

In (15) and (16), ω_c is a characteristic frequency, which is defined based on μ, a, and the soil density ρ as:

$$\omega_c = \sqrt{4\mu/(\rho a^2)}\,. \tag{18}$$

Lam'e constants are related to the modulus of elasticity E (Young's modulus) and Poisson's ratio ν by:

$$\lambda = \frac{\nu E}{(1+\nu)(1-2\nu)}\,,\quad \mu = \frac{E}{2(1+\nu)} \tag{19}$$

The values of modulus of elasticity, E, is provided in Table III for different types of soil [13].

Values of soil density are approximately $1,600$ kg/m^3 when completely dry, and $2,000$ kg/m^3 when completely saturated. Common values for the Poisson's ratio, ν, are in the range from 0.3 (for sand) to 0.5 (for clays, or saturated soils). For our calculations, we select typical values for a medium clay soil and the mass radius of 0.5m. Thus, K and C are calculated as:

$$a = 0.5\,\mathrm{m}\,,\quad \rho = 1,800\,\mathrm{kg/m^3}\,,\quad E = 47,880\,\mathrm{kPa}\,, \tag{20}$$

$$\nu = 0.4\,, \lambda = 68.4\times 10^6 Pa\,,\quad \mu = 17.1\times 10^6 Pa\,, \tag{21}$$

$$n = 2.45\,,\quad \omega_c = 390 s^{-1} \tag{22}$$

$$K = 168.7\times 10^3 \frac{\omega}{tan(\omega/390)}\,,\quad C = 168.7\times 10^3 \tag{23}$$

APPENDIX B
ACKNOWLEDGMENTS

This work is supported by an NSF CAREER award (CNS-0953900). The authors would like to thank Prof. Suat Irmak for his support during the experiments.

REFERENCES

[1] I. F. Akyildiz and E. P. Stuntebeck, "Wireless underground sensor networks: Research challenges," *Ad Hoc Networks*, vol. 4, no. 6, pp. 669 – 686, Nov. 2006.

[2] H. Amick, "A frequency-dependent soil propagation model," in *Proc. SPIE Conference on Current Developments in Vibration Control for Opto-mechanical Systems*, Jul. 1999.

[3] H. R. Bogena and et.al., "Potential of wireless sensor networks for measuring soil water content variability," *Vadose Zone Journal*, vol. 9, no. 4, pp. 1002–1013, November 2010.

[4] D. Castelvecchi, "Wireless energy may power electronics: Dead cell phone inspired research innovation," *MIT TechTalk*, vol. 51, no. 9, Nov. 2006.

[5] X. Dong, M. C. Vuran, and S. Irmak, "Autonomous precision agriculture through integration of wireless underground sensor networks with center pivot irrigation systems," *Ad Hoc Networks Journal*, 2012, accepted for publication. [Online]. Available: http://www.sciencedirect.com/science/article/pii/S1570870512001291

[6] X. Dong and M. C. Vuran, "A channel model for wireless underground sensor networks using lateral waves," in *Proc. IEEE GLOBECOM '11*, Houston, TX, Dec. 2011.

[7] D. Guyomar, G. Sebald, and H. Kuwano, "Energy harvester of 1.5 cm^3 giving output power of 2.6 mw with only 1 g acceleration," *Journal of inteligent material systems and structures*, vol. 22, no. 5, pp. 415–420, Mar. 2011.

[8] A. Karalis, J. Joannopoulos, and M. Soljacic, "Efficient wireless non-radiative mid-range energy transfer," *Elsevier Annals of Physics*, vol. 323, pp. 34–48, Jan. 2008.

[9] A. Kurs, A. Karalis, R. Moffatt, J. D. Joannopoulos, P. Fisher, and M. Soljacic, "Wireless power transfer via strongly coupled magnetic resonances," *Science Journal 6*, vol. 317, no. 5834, pp. 83–86, Jul. 2007.

[10] A. Kurs, R. Moffatt, and M. Soljacic, "Simultaneous mid-range power transfer to multiple devices," *Applied Physics Letters*, vol. 96, no. 044102, Jan. 2010.

[11] E. Lefeuvre, A. Badel, C. Richard, and D. Guyomar, "Piezoelectric energy harvesting device optimization by synchronous electric charge extraction," *Journal of Intelligent Material Systems and Structures*, vol. 16, no. 10, pp. 865 – 876, Oct. 2005.

[12] L. Li, M. Vuran, and I. Akyildiz, "Characteristics of underground channel for wirless underground sensor networks," in *Proc. of IFIP Mediterranean Ad Hoc Networking Workshop (Med-Hoc-Net '07)*, Corfu, Greece, June 2007.

[13] U. A. C. of Engineers, "Settlement analysis," Department of the Army, Tech. Rep. EM 1110-1-1904, Sept. 1990.

[14] G. K. Ottman, H. F. Hofmann, A. C. Bhatt, and G. A. Lesieutre, "Adaptive piezoelectric energy harvesting circuit for wireless remote power supply," *IEEE Trans. on Power Electronics*, vol. 17, no. 5, Sep. 2002.

[15] J. Pan, B. Xue, and Y. Inoue, "A self-powered sensor module using vibration-based energy generation for ubiquitous systems," in *Proc. Int. Conf. ASIC*, Oct. 2005.

[16] S. Roundy, P. Wright, and J. Rabaey, "A study of low level vibrations as a power source for wireless sensor nodes," *Computer Communications Journal*, vol. 26, no. 11, pp. 1131–1144, July 2003.

[17] Y. C. Shu and I. C. Lien, "Analysis of power output for piezoelectric energy harvesting systems," *Smart Material and Structures Journal*, vol. 15, no. 6, pp. 1499–1512, Sep. 2006.

[18] A. R. Silva and M. C. Vuran, "Communication with aboveground devices in wireless underground sensor networks: An empirical study," in *Proc. of IEEE International Conference on Communications (ICC '10)*, Cape Town, South Africa, May 2010, pp. 1–6.

[19] ——, "Empirical evaluation of wireless underground-to-underground communication in wireless underground sensor networks," in *Proc. IEEE DCOSS '09*, Marina del Rey, CA, June 2009.

[20] H. A. Sodano, D. J. Inman, and G. Park, "Generation and storage of electricity from power harvesting devices," *Journal of inteligent material systems and structures*, vol. 16, no. 1, pp. 67–75, Jan. 2005.

[21] D. Strik, H. Hamelers, J. Snel, and C. Buisman, "Green electricity production with living plants and bacteria in a fuel cell," *Int. Journal of Energy Research*, vol. 32, no. 9, pp. 870–876, July 2008.

[22] Z. Sun and I. Akyildiz, "Channel modeling and analysis for wireless networks in underground mines and road tunnels," *IEEE Trans. on Communications*, vol. 58, no. 6, pp. 1758 – 1768, June 2010.

[23] J. Tooker and M. C. Vuran, "Mobile data harvesting in wireless underground sensor networks," in *Proc. IEEE SECON'12*, Seoul, Korea, June 2012.

[24] A. Verruijt, *An Introduction to Soil Dynamics*. Springer Netherlands, 2006, vol. 24.

[25] M. C. Vuran and I. F. Akyildiz, "Channel model and analysis for wireless underground sensor networks in soil medium," *Physical Communication*, vol. 3, no. 4, pp. 245–254, December 2010.

[26] Y. Yang and L. Tang, "Equivalent circuit modeling of piezoelectric energy harvesters," *Journal of inteligent material systems and structures*, vol. 20, pp. 2223– 2235, Dec. 2009.

[27] G. Ye, J. Yan, Z. J. Wong, K. Soga, and A. Seshia, "Optimization of a piezoelectric system for energy harvesting from traffic vibrations," in *IEEE International Ultrasonics Symposium*, Rome, Italy, Sep. 2009.

[28] X. Yu, P. Wu, W. Han, and Z.Zhang, "Overview of wireless underground sensor networks for agriculture," *African Journal of Biotechnology*, vol. 11, pp. 3942–3948, Feb. 2012.